The magnetic instability of $Yb_2Pd_2(In,Sn)$ in a non-Fermi liquid environment

2005 J. Phys.: Condens. Matter 17 S999

(http://iopscience.iop.org/0953-8984/17/11/032)

INSTITUTE OF PHYSICS PUBLISHING JOURNAL OF PHYSICS: CONDENSED MATTER

J. Phys.: Condens. Matter **17** (2005) S999–S1009 doi:10.1088/0953-8984/17/11/032

The magnetic instability of $Yb_2Pd_2(In, Sn)$ in a non-Fermi liquid environment

E Bauer[1,10], G Hilscher[1], H Michor[1], Ch Paul[1], Y Aoki[2], H Sato[2], D T Adroja[3], J-G Park[4], P Bonville[5], C Godart[6,7], J Sereni[8], M Giovannini[9] and A Saccone[9]

[1] Institute of Solid State Physics, Vienna University of Technology, A-1040 Wien, Austria
[2] Department of Physics, Tokyo Metropolitan University, Tokyo 192-0397, Japan
[3] ISIS Facility, Rutherford Appleton Laboratory, Chilton, Didcot, Oxon OX11 0QX, UK
[4] Department of Physics and Institute of Basic Science, Sungkyunkwan University, Suwon 440-746, Korea
[5] CEA, CE Saclay, DSM/DRECAM/SPEC 91191, GIF-SUR-YVETTE, France
[6] CNRS-UPR209, ISCSA, 2-8 rue Henri Dunant, F94320 Thiais, France
[7] LURE, CNRS, Universite Paris Sud, 91405 Orsay, France
[8] Laboratorio Bajas Temperaturas, Centro Atómico Bariloche (CNEA), 8400 SC de Bariloche, Argentina
[9] Department of Chemistry, University of Genova, I-16146 Genova, Italy

E-mail: bauer@ifp.tuwien.ac.at

Received 5 January 2005
Published 4 March 2005
Online at stacks.iop.org/JPhysCM/17/S999

Abstract

Various concentrations of the solid solution $Yb_2Pd_2In_{1-x}Sn_x$ ranging from $x = 0$ to 1 with the tetragonal Mo_2FeB_2-type structure were prepared and their physical properties were studied by means of bulk and spectroscopic measurements as a function of temperature, pressure and magnetic fields. Results deduced from these studies indicate a slight variation of the valency of the Yb ions, from $\nu \approx 2.9$ for both border compounds to $\nu = 3$ at $x = 0.6$. This variation gives rise to the appearance of long range magnetic order in a narrow concentration region around $x = 0.6$, while both border compounds remain non-magnetic. The outstanding concentration dependence for the ordered regime may be indicative of two quantum critical points, a novel feature not yet observed in Yb compounds.

(Some figures in this article are in colour only in the electronic version)

1. Introduction

Yb compounds represent an important class of materials allowing detailed studies of ground state properties arising from mutual interactions such as the Kondo effect, crystal field splitting

[10] Author to whom any correspondence should be addressed.

and RKKY interactions. Additionally, such systems frequently respond in a certain symmetric manner to external parameters such as substitution, pressure or magnetic fields, when compared to isomorphous Ce compounds.

In a number of recent investigations we have explored the physical properties of RE_2Pd_2In with RE = rare earth [1]. Depending on the particular rare earth element, antiferromagnetism occurs with different propagation vectors. For Ce_2Pd_2In, however, ferro- as well as antiferromagnetism can be observed, critically depending on slight changes in stoichiometry [2]. In contrast, long range magnetic order is absent in Yb_2Pd_2In [3, 4]. Physical quantities such as the temperature-dependent electrical resistivity and the specific heat reveal clear signatures of systematic deviations from a Fermi-liquid ground state [4, 5]. The aim of the present work is to trace the evolution of ground state properties of Yb_2Pd_2In with In being substituted by Sn. Such a substitution is expected to influence both the electronic structure and the unit cell volume of this series, since In and Sn are non-isoelectronic elements.

2. Experimental details

Polycrystalline samples of the series $Yb_2Pd_2In_{1-x}Sn_x$ were prepared from stoichiometric amounts of elements by high frequency melting the constituent materials in a closed tantalum crucible. A subsequent heat treatment at 1250 K for one week served to ensure phase purity. All the compounds in the series crystallize with the D^5_{4h} tetragonal space group, and the 4h site occupied by Yb has a low *mm* point symmetry. X-ray diffraction (XRD) and electron microprobe (EPMA) proved the quality of the samples used in the present investigation. Standard techniques have been used to derive the temperature-, field- and pressure-dependent resistivity, the temperature-dependent specific heat and susceptibility as well as isothermal magnetization. Details concerning these techniques are given e.g. in [6]. X-ray absorption (XAS) measurements were performed at the French synchrotron radiation facility (LURE) at Orsay using the x-ray beam of the DCI storage ring (working at 1.85 GeV and 320 mA) on the EXAFS D21 station. The Mössbauer spectroscopy data on the isotope ^{170}Yb ($I_g = 0$, $I_e = 2$, $E_\gamma = 84.3$ keV) were recorded in a standard ^{4}He cryostat using a neutron activated Tm^*B_{12} γ-ray source. Neutron inelastic scattering measurements were performed using the HET time-of-flight spectrometer at the ISIS pulsed neutron source.

3. Results

3.1. Lattice parameters

The evolution of the lattice parameters and of the unit cell volume is displayed in figure 1. The substitution of In by Sn in Yb_2Pd_2In leaves the crystal structure unchanged; the unit cell volume, however, decreases from Yb_2Pd_2In up to about $x = 0.8$ and then increases slightly up to Yb_2Pd_2Sn. Obviously, the concentration dependence does not simply obey Vegard's rule, which may be caused, at least partly, by the non-isoelectronic nature of the In/Sn substitution. Additionally, it is well known that modifications of the valence state of the Yb ion may drive changes of the unit cell volume [7]. Initially, the observed change of the unit cell volume brings about increased chemical pressure onto Yb atoms. This generally causes an enhancement of the magnetic state of Yb with the electronic configuration (EC) approaching the $4f^{13}$ state, while the Kondo interaction is expected to weaken. The final increase of the unit cell volume when approaching Yb_2Pd_2Sn should then recover a state of Yb where Kondo interactions dominate over the tendency of magnetic order.

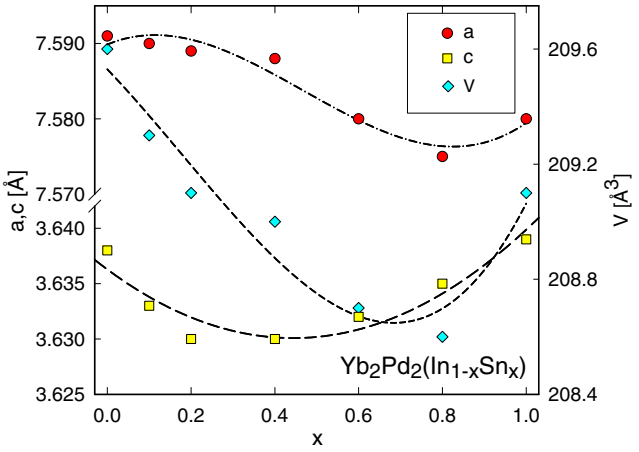

Figure 1. Concentration-dependent lattice parameters a and c and unit cell volume V of $Yb_2Pd_2In_{1-x}Sn_x$. The curves are guides to the eyes.

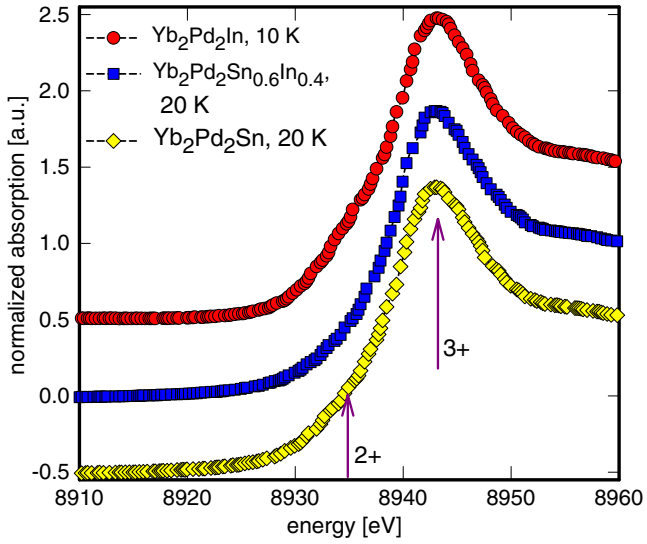

Figure 2. XAS spectra of various concentrations x of $Yb_2Pd_2In_{1-x}Sn_x$ depicted at low temperature.

3.2. L_{III} absorption edge measurements

To explore the electronic state and the thermal stability of Yb in $Yb_2Pd_2In_{1-x}Sn_x$, L_{III} absorption edge measurements were performed for concentrations $x = 0, 0.6$ and 1 at two different temperatures (300 K and 10 or 20 K). The results of the low temperature measurements are shown in figure 2. The larger peak in the spectra at 8943 eV corresponds to the $4f^{13}$ (Yb^{3+}) electronic configuration and the smaller one at 8935 eV to the $4f^{14}$ (Yb^{2+}) state. After subtraction of the background, the L_{III}-edge was decomposed into two peaks in a standard manner [8] yielding $\nu = 2.89(3)$ at $T = 10$ K for Yb_2Pd_2In; a similar result with $\nu = 2.91(3)$ at $T = 20$ K was obtained for Yb_2Pd_2Sn, with only very weak changes with respect to temperature. It is well known that Yb systems exhibiting valencies of about 2.9 or smaller

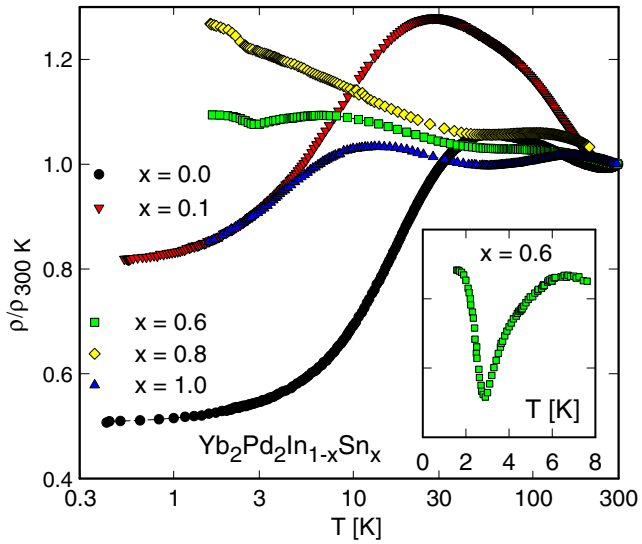

Figure 3. Temperature-dependent resistivity ρ for various concentrations x of $Yb_2Pd_2In_{1-x}Sn_x$ plotted in a normalized representation. The inset shows $\rho(T)$ of $x = 0.6$ at low temperatures.

never show long range magnetic order (compare e.g. [9]). The situation is different for the case $x = 0.6$, where no measurable contribution of the $4f^{14}$ configuration in the experimental L_{III}-edge spectra is observed both at 300 and 20 K, thus revealing a valency $\nu = 3$. Consequently, magnetic order can be expected in this case.

3.3. Electrical resistivity

The scenario already derived for the evolution of physical properties when proceeding from Yb_2Pd_2In to Yb_2Pd_2Sn is well reflected by the development of the temperature-dependent electrical resistivity $\rho(T)$ (see figure 3). Starting with the sample for $x = 0$, one broad maximum is observed around $T_\rho^{\max} \approx 55$ K. Below the maximum, $\rho(T)$ drops markedly to roughly half of the room temperature value without showing a T^2 behaviour of a Fermi liquid state at low temperature. Increasing the Sn content causes three different features: (i) $T_\rho^{\max}$ initially decreases with increasing x, (ii) a high temperature local maximum becomes evident which can be interpreted in terms of crystal field splitting in the presence of the Kondo effect, and (iii) an anomaly develops at low temperatures (see the inset of figure 3 for $x = 0.6$) which can be easily interpreted as the onset of long range magnetic order due to superzone boundary effects [10]. The onset of magnetic order appears to be concentration dependent and is evident for $x = 0.6$ and 0.8 at $T_{\mathrm{mag}} = 2.9$ and 2.5 K, respectively. However, as x is further increased towards $x = 1$, the distinct features of long range magnetic order vanish again. The existence of the magnetic order is also clearly proven by our subsequent specific heat and Mössbauer spectroscopy data (see below).

A characteristic feature of a Kondo lattice is a maximum in ρ versus T at $T = T_\rho^{\max}$, which can be taken as a measure of the Kondo temperature T_{K} [11]. The concentration dependence of the characteristic temperatures is summarized in figure 10. Similar to the concentration-dependent evolution of the lattice parameters, $T_\rho^{\max}$ changes in a non-monotonic manner, reaching the lowest value around the concentration where the long range magnetic order begins. Below and above these concentrations $T_\rho^{\max}$ becomes significantly larger. Since the

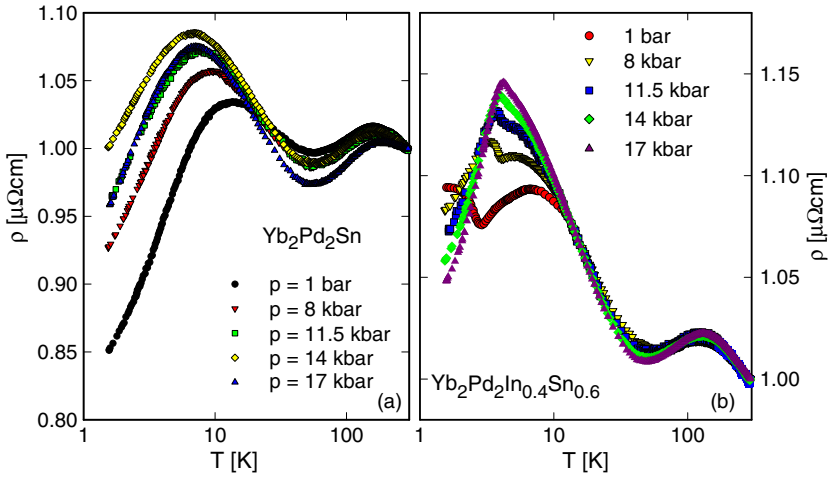

Figure 4. Temperature- and pressure-dependent resistivity ρ of (a) Yb_2Pd_2Sn and (b) $Yb_2Pd_2In_{0.4}Sn_{0.6}$ plotted in a normalized representation.

RKKY scale is expected to exceed the Kondo scale at the region where a long range magnetic order is observed, $T_\rho^{\max}$ may not be directly considered as T_K.

In an attempt to disentangle the different energy scales, pressure-dependent measurements of the electrical resistivity were carried out for various concentrations of the series. Some typical examples of these measurements are shown in figure 4 for concentrations $x = 0.6$ and 1. While for the latter $T_\rho^{\max}$ decreases as the pressure increases—in good agreement with observations made for Yb compounds in general—the maxima observed in $\rho(T)$ for the sample $x = 0.6$ behave in a much more complicated way (see figure 4(b)). While the anomaly associated with the onset of magnetic order seems to increase with pressure, the broader maximum at higher temperature in ρ versus T moves slightly towards low temperature and finally flattens out. This may indicate that for this particular case T_K can no longer be taken from $T_\rho^{\max}$ in the resistivity data.

The field response of the temperature-dependent electrical resistivity has been investigated for the present series; data for $Yb_2Pd_2In_{0.2}Sn_{0.8}$ are plotted in figure 5 for $H \perp I$. $Yb_2Pd_2In_{0.2}Sn_{0.8}$ exhibits a negative magnetoresistance throughout the field and temperature range studied here which amounts to about 25% at the extreme borders. The most interesting feature is the suppression of the anomaly around the onset of long range magnetic order. This observation can be taken as an almost unambiguous signature of antiferromagnetic ordering. The critical field is estimated to be about 3 T. At low temperature, resistivity data taken from the 4 T run is proportional to $T^{1.2}$, indicating a field derived non-Fermi liquid state. As the field strength increases, the local maximum shifts towards higher temperatures, and at a field of 12 T a Fermi liquid ground state is recovered, evidenced from the T^2 behaviour of $\rho(T)$ at low temperatures.

3.4. Magnetic susceptibility

The temperature-dependent magnetic susceptibility of $Yb_2Pd_2In_{1-x}Sn_x$ is shown in figure 6 for various samples of the series. At temperatures above about 50 K, the data were analysed in terms of a modified Curie–Weiss law. The results of least squares fits reveal magnetic moments of 3.88, 4.16 and 3.64 μ_B/Yb and paramagnetic Curie temperatures of -69, -24

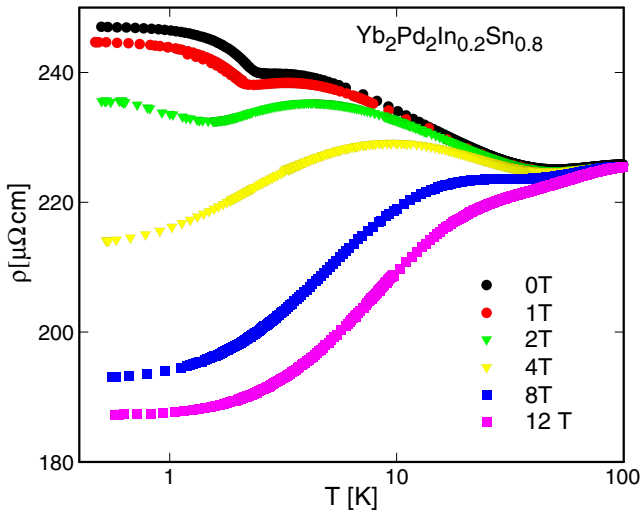

Figure 5. Temperature-dependent resistivity ρ of $Yb_2Pd_2In_{0.2}Sn_{0.8}$ measured at various magnetic fields.

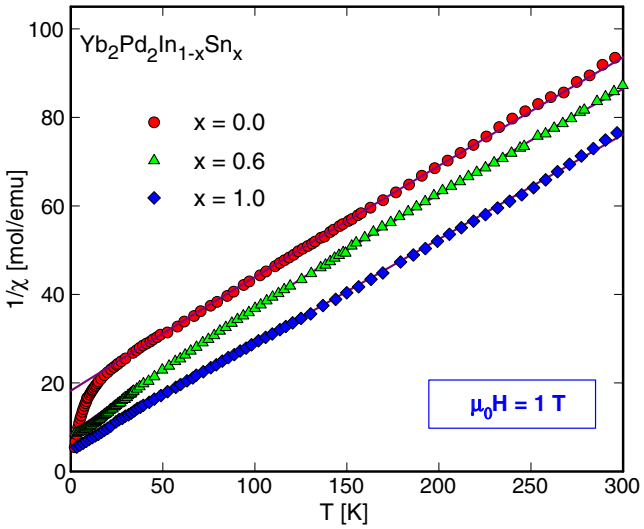

Figure 6. Temperature-dependent inverse susceptibility $1/\chi$ for various concentrations x of $Yb_2Pd_2In_{1-x}Sn_x$. The solid lines are least squares fits according to the modified Curie–Weiss law.

and -29 K, for $x = 0, 0.6$ and 1, respectively. The effective magnetic moments observed are found to be smaller than the value 4.54 μ_B of Yb^{3+}, and are even lower than the value inferred from a valence state of about 2.9 for $x = 0$ and 1. The differences of both specimens with respect to $x = 0.6$ scales, however, with the differences found in the respective valence states. The paramagnetic Curie temperatures are large and negative, pointing to pronounced antiferromagnetic interactions. Besides the Kondo effect, which causes a moment reduction, in agreement with the negative Curie temperatures and the logarithmic contribution to the electrical resistivity, crystal field splitting is another possible mechanism which may modify

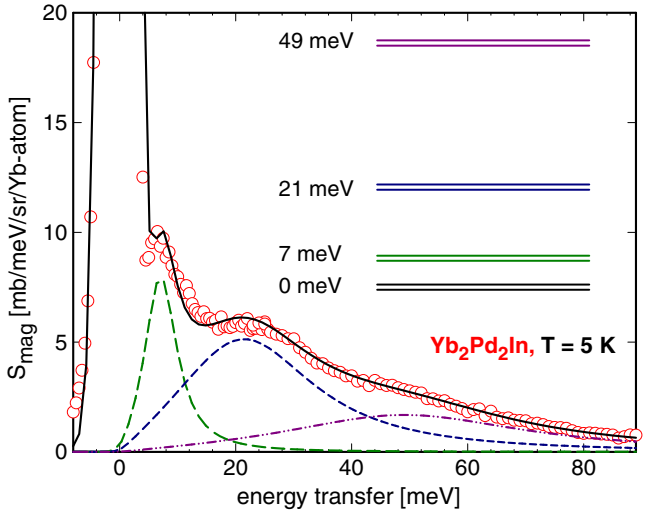

Figure 7. Inelastic neutron scattering spectrum of Yb_2Pd_2In at $T = 5$ K. The dashed lines account for Lorentzian-type peaks centred at 7, 21 and 49 meV and the solid line is for the total scattering. The crystal field level scheme inferred from these data is sketched in this figure additionally.

the effective magnetic moment of the Yb ions. In fact, if the overall crystal field splitting increases, the effective moment may decrease under certain circumstances. In order to estimate the crystal electric field splitting, inelastic neutron scattering measurements were performed with different neutron incident energies at various temperatures.

3.5. Inelastic neutron scattering

Figure 7 shows the magnetic part of the inelastic spectrum from Yb_2Pd_2In, measured using the HET spectrometer with the incident neutron energy $E_i = 100$ meV at an average scattering angle of 19° at $T = 5$ K. The phonon scattering was subtracted by measuring the isostructural non-magnetic reference compound Lu_2Pd_2In with identical conditions. The magnetic scattering function can be decomposed into one quasielastic and three inelastic lines, resulting from crystal electric field excitations. The latter originate from the partial lifting of the eight-fold degeneracy of the Yb^{3+} spin–orbit ground state, with total angular momentum $J = 7/2$, in the crystal field with *mm* symmetry at the Yb site. Thus one expects three crystal field excitations in addition to a quasielastic excitation near zero energy transfer. The centre of the inelastic lines yields then the first excited doublet above the ground state at 7 meV, the second one at 21 meV and the uppermost doublet at 49 meV. In stable magnetic systems, the linewidth should be resolution limited (the instrument resolution with $E_i = 100$ meV is FWHM ≈ 5.6 meV at elastic energy and about 1.8 meV at 80 meV energy transfer). Kondo interaction, however, significantly broadens the inelastic transition, which furthermore increases with increasing temperature. It is interesting to note that despite the decrease of the instrument resolution with increasing energy transfer, the linewidth of the crystal field excitations increases significantly with energy transfer. The rather large overall crystal field splitting with broader linewidth in conjunction with Kondo interaction might well explain the fact that the effective magnetic moments (deduced from the susceptibility below room temperature) found throughout the series are well below $\mu_{eff} = 4.54\ \mu_B$. As the Yb, Pd and In ions occupy different (but unique) crystallographic sites in the Mo_2FeB_2-type

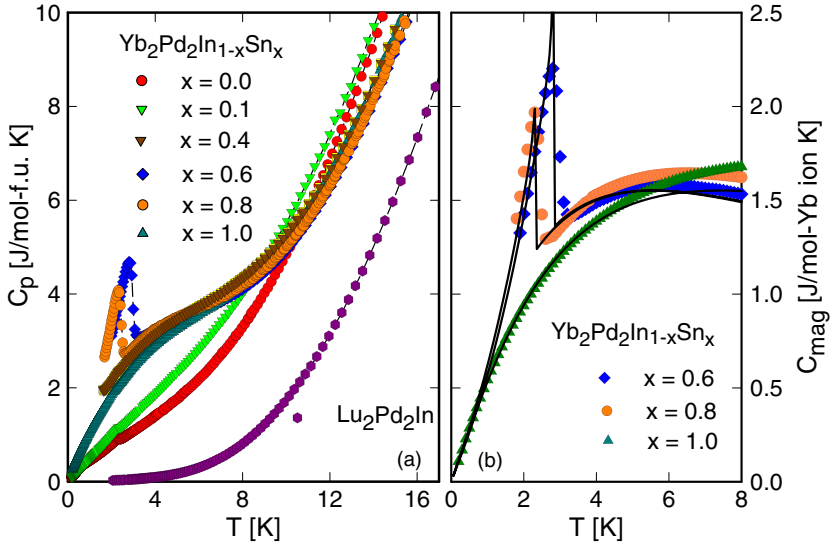

Figure 8. (a) Temperature-dependent specific heat C_p for various concentrations of $Yb_2Pd_2In_{1-x}Sn_x$ in units referring to one formula unit. (b) Temperature-dependent magnetic contribution to the specific heat $C_{\rm mag}$ of $x = 0.6$, 0.8 and 1.0 in units referring to one Yb ion. The solid lines are fits according to the Kondo model in the presence of long range magnetic order.

structure, the broadening of the CEF excitations could not be due to the disordering effect. We therefore attribute the broadening of the CEF excitations in Yb_2Pd_2In to a possibly strong and especially preferential mixing between 4f CEF wavefunctions with the conduction electron wavefunctions.

3.6. Specific heat

In order to investigate the ground state properties of this series in more detail, specific heat measurements, $C_p(T)$, were performed; the results are shown in figure 8(a) together with non-magnetic Lu_2Pd_2In ($\theta_D \approx 190$ K). $C_p(T)$ for concentrations $x = 0$, 0.1 and 1 was measured down to the 100 mK range; none of them shows anomalies indicative of a long range magnetic order. Samples with $x = 0.6$ and 0.8, however, exhibit λ-like anomalies, evidencing a long range magnetic order. It is unusual that although a magnetically ordered ground state is not found for one of the border compounds, magnetic ordering develops in a narrow concentration range at the Sn-rich region. These observed features are in perfect agreement with the resistivity data discussed above.

Low temperature details of the specific heat are displayed in figure 8(b) as $C_{\rm mag}$ versus T for concentrations $x = 0.6$, 0.8 and 1. $C_{\rm mag}$ is obtained from a comparison of the Yb-based samples with the respective data of non-magnetic Lu_2Pd_2In. Again, magnetic phase transitions are clearly seen for $x = 0.6$ and 0.8, while the border compound Yb_2Pd_2Sn stays non-magnetic, at least down to 100 mK. While, however, in a mean field type of magnetic phase transition the jump of the specific heat at $T = T_{\rm ord}$ is about 12.5 J mol^{-1} K^{-1} in the case of a doublet ground state, Kondo interaction may cause a substantial reduction depending on the ratio T_K/T_{RKKY}. Here, $k_B T_K$ is the Kondo interaction strength and $k_B T_{RKKY}$ measures the inter-site interaction responsible for long range magnetic order. Beyond a critical value of T_K/T_{RKKY} long range magnetic order vanishes; hence, an anomaly can no longer be deduced from the experimental

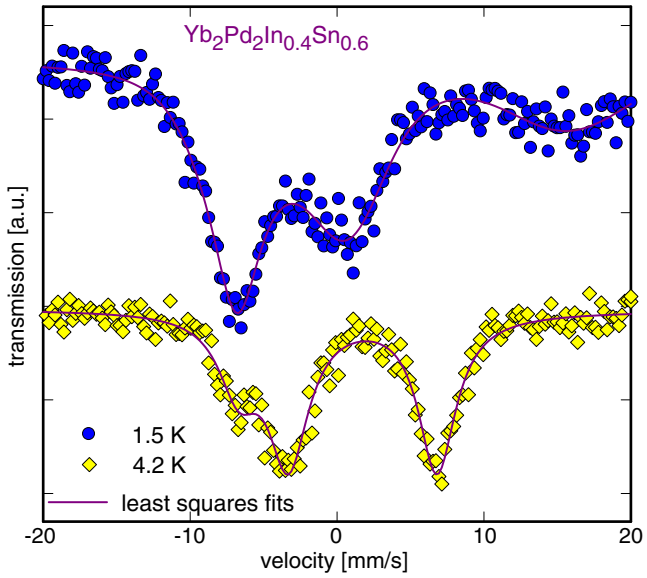

Figure 9. ^{170}Yb Mössbauer spectra at 1.5 and 4.2 K of $Yb_2Pd_2In_{1-x}Sn_x$.

data. In order to quantitatively account for the observed behaviour we made calculations using the mean field model for long range magnetic order [12] together with the model of Schotte and Schotte [13], which then allows us to trace the temperature-dependent specific heat only using two adjustable parameters: T_K and T_{RKKY}. The results of such a fitting procedure are displayed in figure 8(b) as solid lines. The Kondo temperatures deduced thereby amount to about 11, 12 and 15 K for $x = 0.6$, 0.8 and 1, respectively. For $x = 0.6$ and 0.8, the RKKY interaction strength is about twice the Kondo interaction, which—in that model—would lead to magnetic ordering around 10 K, if the Kondo effect were absent. For the case of $x = 1$, T_{RKKY} does not influence the shape of the specific heat curve, as long as the non-magnetic condition of T_K/T_{RKKY} is fulfilled. Deviations of the fit from data at higher temperatures may result from additional crystal field contributions and/or from the uncertainties in defining $C_{mag}(T)$. The fitting curves in figure 8(b) also allow the determination of the Sommerfeld value γ, yielding 550, 505 and 560 mJ/(mol-Yb K^2), for $x = 0.6$, 0.8 and 1, respectively. A comparison with T_K contrasts the widespread assumption that $T_K \propto 1/\gamma$. Rather, γ is not only dependent on T_K, but is intimately related to T_{RKKY} as well, at least as long as T_K/T_{RKKY} stays within a magnetic solution.

3.7. Mössbauer spectroscopy

^{170}Yb Mössbauer spectra have been recorded for $x = 0$, 0.6 and 1. Spectra at 1.5 and 4.2 K are shown here for the concentration $x = 0.6$ in figure 9. For this concentration, the data evidence the presence of magnetic ordering at 1.5 K: the spectrum at this temperature shows indeed a magnetic hyperfine field (about 100 T) at the nucleus site, whereas the spectrum at 4.2 K is a pure quadrupolar hyperfine spectrum characteristic of the paramagnetic phase. The hyperfine field observed at 1.5 K corresponds to a spontaneous Yb moment $\mu_s \approx 1\ \mu_B$. The most energetic line of this spectrum is very broad, which indicates a rather large distribution of hyperfine fields, probably due to the statistical distribution of In and Sn in the lattice.

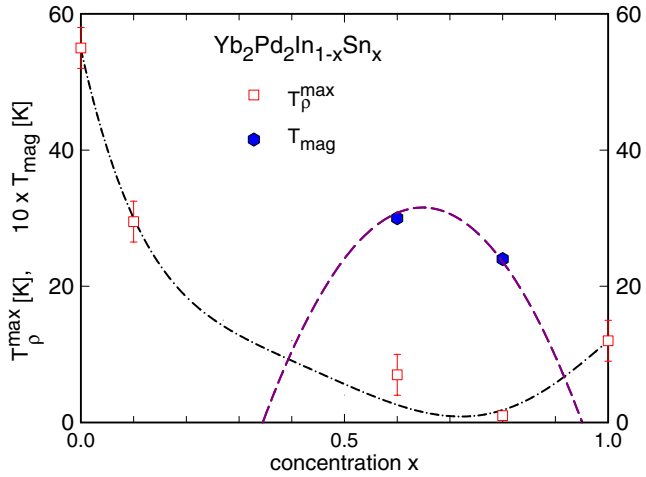

Figure 10. Phase diagram of $Yb_2Pd_2In_{1-x}Sn_x$. T_ρ^{max} is the maximum temperature deduced from the electrical resistivity and T_{mag} is the magnetic ordering temperature. The dashed and the dashed–dotted curves are guides to the eyes.

This spectrum is a further confirmation that the anomalies in $\rho(T)$ and $C_p(T)$ correspond to magnetic transitions, at least for $x = 0.6$.

4. Discussion and summary

The ground state properties of $Yb_2Pd_2In_{1-x}Sn_x$ obviously evolve in a non-monotonic manner. In terms of a rigid band model of such compounds the In/Sn substitution causes an increase of the electron count, and consequently the Fermi level may be driven towards higher energies. This resulting Fermi level tuning can then be considered as a primary mechanism provoking the observed change of the ground state properties throughout the series. The non-monotonic change would be a consequence of a non-monotonic variation of the DOS within the range of the shift of the Fermi energy. Additional chemical pressure due to the variation of the unit cell volume may also help significant variations of the electronic structure.

The electronic-driven modifications of physical properties upon the In/Sn substitution is clearly evidenced from a change of characteristic energy scales (see figure 10). Taking into account the characteristic temperature T_ρ^{max} derived from the resistivity measurements, the Kondo temperature T_K of a Kondo lattice is estimated from $T_\rho^{max} \propto T_K$ [11]. Such an estimate would give $T_K \approx 55$ K for Yb_2Pd_2In. One should note, however, that this model applies just for those cases where the Kondo scale by far dominates over all other mechanisms such as the RKKY interaction or crystal field splitting. Within this scenario, the pressure response is large and a significant change of T_ρ^{max} can be expected. In fact, T_ρ^{max} of $x = 0$ alters by more than 50% in the pressure range of up to 16 kbar. It thus appears that T_K is the dominating scale [4]. All other compounds exhibit a much smaller variation of $\partial T_\rho^{max}/\partial p$, indicating the growing importance of RKKY interaction and crystal field splitting. Nevertheless, the $T_\rho^{max}(x)$ dependence points at small T_K values in the Sn-rich region for concentrations well below $x = 1$. In fact, analyses of the specific heat data corroborate this assumption. T_K is expected to become smaller in the Sn-rich region, well below $x = 1$. The physical properties in this region are indicative of long range magnetic order; the latter is stabilized by the low T_K values within this concentration range. A presumption concerning the nature of the ordered magnetic

moments cannot totally exclude certain forms of an antiferromagnetic spin-density wave. The fact that ordering is constrained within a narrow—yet not fully determined—concentration range provides the possibility of having two quantum critical points within a single series. This would be a novel feature of Yb compounds and would allow us to study quantum phase transitions in different environments, i.e., different ratios of the Kondo temperature, RKKY interaction and crystal field splitting. Pronounced deviations from a Fermi liquid ground state were already noticed from resistivity and specific heat measurements for compounds outside the magnetically ordered region. Some details of these features were discussed in [4, 5].

In summary, In/Sn substitution in ternary Yb_2Pd_2In causes non-monotonic modifications of physical properties throughout the series. Within a limited Sn-rich region, the Yb ions approach the trivalent state, providing the condition to stabilize long range magnetic order.

Acknowledgments

This work was supported by the Austrian FWF P16370 and P15066. We acknowledge the Austrian-French Amadeus Program 05545RE. Work at Sungkyunkwan University was supported by the Proton Accelerator User Program (No. M102KS010001-02K1901-01810) of Proton Engineering R&D Project of the Ministry of Science and Technology. Experiments at ISIS were supported by the Engineering and Physical Sciences Research Council of the UK. We thank S Sanada for his technical assistance.

References

[1] Fischer P, Herrmannsdörfer T, Bonelli T, Fauth F, Keller L, Bauer E and Giovannini M 2000 *J. Phys.: Condens. Matter* **12** 7089
[2] Giovanni M, Michor H, Bauer E, Hilscher G, Rogl P, Fischer P, Bonelli Th, Fauth F, Hermannsdörfer Th, Keller L, Saccone A and Ferro R 2000 *Phys. Rev.* B **61** 4044
[3] Giovannini M, Bauer E, Michor H, Hilscher G, Galatanu A, Saccone A and Rogl P 2001 *Intermetallics* **9** 481
[4] Bauer E, Berger St, Gabani S, Hilscher G, Michor H, Paul Ch, Giovannini M, Saccone A, Godart C, Bonville P, Aoki Y and Sato H 2003 *Acta Phys. Pol.* B **34** 367
[5] Bauer E, Hilscher G, Michor H, Paul Ch, Aoki Y, Sato H, Giovannini M and Saccone A 2004 *J. Magn. Magn. Mater.* **272–276** 237
[6] Bauer E, Berger St, Paul Ch, Della Mea M, Hilscher G, Michor H, Reissner M, Steiner W, Grytsiv A, Rogl P and Scheidt E W 2002 *Phys. Rev.* B **66** 214421
[7] Neumann G, Pott R, Rohler J, Schlabitz W, Wohlleben D K and Zahel H 1982 *Proc. Int. Conf. on Valence Instabilities (Zürich, 1982)* ed P Wachter and H Boppart (Amsterdam: North-Holland)
[8] Godart C, Achard J C, Krill G and Ravet-Krill M F 1983 *J. Less-Common Met.* **94** 177
[9] Bauer E, Hauser R, Keller L, Fischer P, Trovarelli O, Sereni J, Rieger J J and Stewart G 1997 *Phys. Rev.* B **56** 711
[10] Meaden G T 1971 *Contemp. Phys.* **12** 313 and references cited therein
[11] Cox D and Grewe N 1988 *Z. Phys.* B **71** 321
[12] Besnus M J, Braghta A, Hamdaoui N and Meyer A 1992 *J. Magn. Magn. Mater.* **104–107** 1385 and references therein
[13] Schotte K D and Schotte U 1975 *Phys. Lett.* A **55** 38